# Global instability and control of laminar separation bubbles : Theoretical background, basic flow documentation, algorithmic developments and validation

**Vassilis THEOFILIS**

*School of Aeronautics, Universidad Politécnica de Madrid,*
*Pza. Cardenal Cisneros 3, E-28040 Madrid, Spain*

**Abstract.** Elements of the theoretical foundation for control of local and global instabilities in laminar separation bubble (LSB) flows are presented. The classic decelerated boundary layer of Howarth [12, 13] in which BiGlobal eigenmodes of separated flow were first discovered [21] is revisited. A systematic investigation covering the Reynolds number range $Re \in [10^3, 10^5]$ has been performed and has revealed the boundary between steady- and time-periodic (shedding) basic LSB flows. Validation solutions of the adjoint BiGlobal eigenvalue problem are then presented and first steps toward massively parallel solution of both the direct and the adjoint BiGlobal EVP are discussed.

**Key words:** Incompressible LSB, Direct/Adjoint BiGlobal EVP, DNS, parallel Arnoldi algorithm

## 1. Introduction

The seminal work of Briley [4] demonstrated that direct numerical simulation (DNS) of the full Navier-Stokes equations confines the (in)famous Goldstein singularity, associated with Howarth's [12] decelerated boundary layer, within the realm of numerical solutions of the non-interactive, non-similar boundary-layer equations. Briley resolved the full equations of motion on a flat plate, within a domain $\{[x_1, x_2] \times [0, y_\infty]\}$ in the streamwise, $x$, and wall–normal, $y$, spatial directions, respectively. In the far-field he imposed Howarth's free-stream velocity distribution

$$\bar{u}(x, y \to \infty) = \begin{cases} \beta_0 - \beta_1 x & x_1 \leq x \leq x_0, \\ \beta_0 - \beta_1 x_0 & x_0 \leq x \leq x_2, \end{cases} \tag{1}$$

using $x_0$ as a free parameter to control the extent of the linear deceleration region, and was capable to recover steady laminar separated bubbles embedded inside boundary layer flows. In this context, the parameter $\beta_0$ corresponds to the (dimensional) free-stream velocity which, together with the deceleration parameter $\beta_1$, may be used in order to build a length scale, $\beta_0/\beta_1$; in turn, the free-stream velocity, this length scale and the flow kinematic viscosity $\nu$ may be used to define the flow Reynolds number

$$Re = \frac{\beta_0^2}{\beta_1 \nu}. \tag{2}$$

In the multi-parametric problem at hand (and no doubt on account of the limited computing capabilities of that time) Briley [4] mainly concentrated on the effect of $x_0$ on the LSB at a few representative values of the Reynolds number.

About a decade ago, Theofilis [21] and Theofilis, Hein & Dallmann [27] have recovered steady LSB flows using Howarth's model and DNS, and went on to analyze these flows with respect to their local and global instability properties. While evidence on the existence of global modes in model separated flows was already available – albeit using a methodology which relies on the assumption of weakly-nonparallel basic flow [2, 10] – of particular interest in [21, 27] was the first application of the BiGlobal eigenvalue problem (EVP) concept and the subsequent discovery of amplified three-dimensional global modes of LSB flows. The key difference between [21, 27] and [2, 10] is that the BiGlobal methodology permits instability analysis of arbitrary two–dimensional basic states, and has indeed been used since in several applications of engineering significance in which LSB appear; see [22] for a discussion. No parametric BiGlobal EVP studies were performed in [21, 27], since the serial solution methodology followed required state-of-the-art supercomputing facilities of that era, in order for convergence of the eigenspectrum results to be attained. Using the same incompressible BiGlobal EVP approach, Robinet and Joubert de la Motte [18] have confirmed the global modes found in [21, 27] and have also identified three-dimensional amplified global modes in different incompressible LSB flows. Recently, Robinet [17] has discovered BiGlobal instabilities in LSB flows which result from shock/boundary-layer interaction. In all cases studied so far, BiGlobal instability of LSB flows is a feeble modal mechanism, which may co-exist with the well-known and order-of-magnitude stronger Kelvin-Helmholtz (KH) inviscid instability associated with the inflectional nature of the shear-layer profile. Nevertheless, in the light of the discovery of global modes in LSB flows, flow control methodologies aiming at flow modifications through control of modal instabilities need to take both the local and the global instability mechanisms into consideration.

The present contribution continues the renewed efforts, which have commenced recently [24], on the systematic characterization and control of modal instability mechanisms in LSB flows. Initially, elements of the theoretical foundation of the flow control problem are discussed [7, 9] and the direct and adjoint BiGlobal eigenvalue problems are defined. The BiGlobal methodology, as opposed to EVPs of the Orr-Sommerfeld class [11], has been chosen here, since it encompasses results of the latter methodology in LSB flows [19, 24] and has also been demonstrated to be appropriate for the related attached boundary–layer problem [7, 16]. Subsequently, attention is turned to the underlying basic states; the well-documented and relevant to external aerodynamics decelerating boundary–layer model of Howarth [12] is used in order to impose the adverse pressure gradient; in this context, the boundaries of the parameter space within which steady bubbles exist are documented in the range $Re \in [10^3, 10^5]$, as are integral flow quantities, such as the thickness of the incoming boundary layer and the maximum absolute value of the reverse flow. [1] Finally, attention is turned to the EVPs and the numerical solution of the adjoint BiGlobal EVP is validated on a flow case that is well-documented and less-challenging from a resolution requirements point of view. On the other hand, accurate description of convective BiGlobal eigenmodes of LSB flow [24] renders the commonly used serial solutions of the BiGlobal EVP problems inadequate; a discussion of pivotal developments toward efficient massively parallel solution of the BiGlobal EVPs closes the present contribution.

[1] characterization of the bubbles themselves is still an open question [8, 6]

## 2. Theoretical Background: the incompressible direct and adjoint BiGlobal EVPs

The (direct) linearized incompressible Navier-Stokes and continuity equations read

$$\frac{\partial \hat{\mathbf{q}}^*}{\partial t} + \mathcal{N}(\bar{\mathbf{q}})\hat{\mathbf{q}}^* + \nabla \hat{p}^* = 0, \tag{3}$$

$$\nabla \cdot \hat{\mathbf{q}}^* = 0. \tag{4}$$

Assuming modal perturbations and homogeneity in the spanwise spatial direction, $z$, eigenmodes are introduced into the linearized direct Navier-Stokes and continuity equations according to

$$(\hat{\mathbf{q}}^*, \hat{p}^*) = (\hat{\mathbf{q}}(x,y), \hat{p}(x,y))\mathrm{e}^{+\mathrm{i}(\beta z - \omega t)}, \tag{5}$$

where $\hat{\mathbf{q}}^* = (\hat{u}^*, \hat{v}^*, \hat{w}^*)^{\mathrm{T}}$ and $\hat{p}^*$ are, respectively, the vector of amplitude functions of linear velocity and pressure perturbations, superimposed upon the steady two-dimensional, two- ($\bar{w} \equiv 0$) or three-component, $\bar{\mathbf{q}} = (\bar{u}, \bar{v}, \bar{w})^T$, steady LSB basic states. The spanwise wavenumber $\beta$ is associated with the spanwise periodicity length, $L_z$, through $L_z = 2\pi/L_z$. Substitution of (5) into (3-4) results in the complex *direct* BiGlobal eigenvalue problem [22]

$$\hat{u}_x + \hat{v}_y + i\beta\hat{w} = 0, \tag{6}$$

$$(\mathcal{L} - \bar{u}_x + \mathrm{i}\omega)\,\hat{u} - \bar{u}_y\hat{v} - \hat{p}_x = 0, \tag{7}$$

$$-\bar{v}_x\hat{u} + (\mathcal{L} - \bar{v}_y + \mathrm{i}\omega)\,\hat{v} - \hat{p}_y = 0, \tag{8}$$

$$-\bar{w}_x\hat{u} - \bar{w}_y\hat{v} + (\mathcal{L} + i\omega)\,\hat{w} - i\beta\hat{p} = 0, \tag{9}$$

where

$$\mathcal{L} = \frac{1}{Re}\left(\frac{\partial^2}{\partial x^2} + \frac{\partial^2}{\partial y^2} - \beta^2\right) - \bar{u}\frac{\partial}{\partial x} - \bar{v}\frac{\partial}{\partial y} - i\beta\bar{w}. \tag{10}$$

The derivation of the complex BiGlobal eigenvalue problem governing adjoint perturbations is constructed using the Euler-Lagrange identity [15, 7, 3, 16, 14, 9],

$$\begin{aligned}\left[\left(\frac{\partial \hat{\mathbf{q}}^*}{\partial t} + \mathcal{N}\hat{\mathbf{q}}^* + \nabla\hat{p}^*\right)\cdot\tilde{\mathbf{q}}^* + \nabla\cdot\hat{\mathbf{q}}^*\tilde{p}^*\right] \quad + \\ \left[\hat{\mathbf{q}}^*\cdot\left(\frac{\partial \tilde{\mathbf{q}}^*}{\partial t} + \mathcal{N}^\dagger\tilde{\mathbf{q}}^* + \nabla\tilde{p}^*\right) + \hat{p}^*\nabla\cdot\tilde{\mathbf{q}}^*\right] \quad = \\ \frac{\partial}{\partial t}\left(\hat{\mathbf{q}}^*\cdot\tilde{\mathbf{q}}^*\right) + \nabla\cdot j(\hat{\mathbf{q}}^*, \tilde{\mathbf{q}}^*),\end{aligned} \tag{11}$$

as applied to the linearized incompressible Navier-Stokes and continuity equations. Here the operator $\mathcal{N}^\dagger(\bar{\mathbf{q}})$ results from linearization of the convective and viscous terms in the direct and adjoint Navier-Stokes equations and is explicitly stated elsewhere (e.g. [7]). The quantities $\tilde{\mathbf{q}}^* = (\tilde{u}^*, \tilde{v}^*, \tilde{w}^*)^{\mathrm{T}}$ and $\tilde{p}^*$ denote adjoint disturbance velocity components and adjoint disturbance pressure, and $j(\hat{\mathbf{q}}^*, \tilde{\mathbf{q}}^*)$ is the bilinear concomitant. Vanishing of the RHS term in the Euler-Lagrange identity (11) defines the adjoint linearized incompressible Navier-Stokes and continuity equations

$$\frac{\partial \tilde{\mathbf{q}}^*}{\partial t} + \mathcal{N}^\dagger\tilde{\mathbf{q}}^* + \nabla\tilde{p}^* = 0, \tag{12}$$

$$\nabla\cdot\tilde{\mathbf{q}}^* = 0, \tag{13}$$

Assuming modal perturbations and homogeneity in the spanwise spatial direction, $z$, eigenmodes are introduced into (12-13) according to

$$(\tilde{\mathbf{q}}^*, \tilde{p}^*) = (\tilde{q}(x,y), \tilde{p}(x,y))\mathrm{e}^{-\mathrm{i}(\beta z - \omega t)}. \tag{14}$$

Note the opposite signs of the spatial direction $z$ and time in (5) and (14), denoting propagation of $\tilde{\mathbf{q}}^*$ in the opposite directions compared with the respective one for $\hat{\mathbf{q}}^*$. Substitution of (14) into the adjoint linearized Navier-Stokes equations (12-13) results in the complex *adjoint* BiGlobal EVP

$$\begin{aligned}
\tilde{u}_x + \tilde{v}_y - \mathrm{i}\beta\tilde{w} &= 0, && (15)\\
\left(\mathcal{L}^\dagger - \bar{u}_x + \mathrm{i}\omega\right)\tilde{u} - \bar{v}_x\tilde{v} - \bar{w}_x\tilde{w} - \tilde{p}_x &= 0, && (16)\\
-\bar{u}_y\tilde{u} + \left(\mathcal{L}^\dagger - \bar{v}_y + \mathrm{i}\omega\right)\tilde{v} - \bar{w}_y\tilde{w} - \tilde{p}_y &= 0, && (17)\\
\left(\mathcal{L}^\dagger + \mathrm{i}\omega\right)\tilde{w} + \mathrm{i}\beta\tilde{p} &= 0, && (18)
\end{aligned}$$

where

$$\mathcal{L}^\dagger = \frac{1}{Re}\left(\frac{\partial^2}{\partial x^2} + \frac{\partial^2}{\partial y^2} - \beta^2\right) + \bar{u}\frac{\partial}{\partial x} + \bar{v}\frac{\partial}{\partial y} - \mathrm{i}\beta\bar{w}. \tag{19}$$

Note also that the two-dimensionality of the LSB basic state implies $\bar{w} \equiv 0$ in both the direct and adjoint EVP, both of which may be reformulated to use real arrays alone [22, 25], thus saving half of the otherwise necessary memory requirements for the coupled numerical solution of the EVPs (6-9) and (15-18).

Boundary conditions for the partial-derivative based adjoint EVP may be devised following the general procedure of expanding the bilinear concomitant in order to capture traveling disturbances [7]. However, here focus is on global modes, which previous investigations have shown to be located in the immediate vicinity of the primary laminar separation bubble [21, 27]. This permits use of simpler set of boundary conditions, as follows. For the direct problem, homogeneous Dirichlet boundary conditions are used at the inflow, $x = x_{IN}$, wall, $y = 0$, and far-field, $y = y_\infty$, boundaries, alongside linear extrapolation at the outflow boundary $x = x_{OUT}$. Consistently, homogeneous Dirichlet boundary conditions at $y = 0$, $y = y_\infty$ and $x = x_{OUT}$, alongside linear extrapolation from the interior of the computational domain at $x = x_{IN}$, are used in order to close the adjoint EVP.

Luchini and co-workers have recently put forward the idea of structural sensitivity of global modal perturbations, which may be identified through a direct-adjoint BiGlobal eigenmode product, and successfully applied the concept to the lid-driven cavity flow [14] and the cylinder wake [9]. The former flow, which shares with the LSB the two-component character of the basic state, has served here for validations of the numerical solution of (15-18); in this case, homogeneous Dirichlet boundary conditions on the adjoint perturbations have been imposed.

### 2.1. Basic Flow Documentation

The LSB basic flow is obtained via two-dimensional DNS, solving simultaneously the vorticity-transport equation, alongside the relationship between vorticity, $\zeta$, and streamfunction, $\psi$,

$$\zeta_t + \psi_y \zeta_x - \psi_x \zeta_y = \frac{1}{Re}\nabla^2 \zeta + \lambda_f(x)(\zeta - Z), \tag{20}$$

$$\nabla^2 \psi + \zeta = \lambda_f(x)(\psi - \Psi). \tag{21}$$

The components of the basic flow velocity vector, $(\bar{u}, \bar{v})^{\mathrm{T}}$, appearing in the EVPs (7-9) and (16-18) may be obtained from $\bar{u} \equiv \partial\psi/\partial y$ and $\bar{v} \equiv -\partial\psi/\partial x$; note also that in the present work $\bar{w} \equiv 0$ is considered. A fringe function, $\lambda(x)$ [20, 26], is used in order to return the flow to its inflow state, $Z$ and $\Psi$, respectively.

Spatial discretization of (20-21) is accomplished by mapped Chebyshev Gauss-Lobatto (CGL) spectral collocation schemes along the wall-normal, $y-$, and streamwise, $x-$, spatial direction. The standard CGL domain,

$$\eta_j = \cos j\pi/N, \quad j = 0, \cdots, N \tag{22}$$

is mapped onto a finite domain, $\xi \in [\xi_{\mathrm{l}}, \xi_{\mathrm{r}}]$ via a rational function

$$\xi = \xi(\eta) = a\frac{1 + b - \eta}{1 + c + \eta}, \tag{23}$$

where

$$a = \frac{-2\xi_{\mathrm{l}}\xi_{\mathrm{r}} + \xi_0\left[\xi_{\mathrm{r}}(1 + \eta_0) + \xi_{\mathrm{l}}(1 - \eta_0)\right]}{\xi_{\mathrm{r}}(1 - \eta_0) + \xi_{\mathrm{l}}(1 + \eta_0) - 2\xi_0}, \tag{24}$$

$$b = \frac{2}{a}\frac{\xi_{\mathrm{l}}(a + \xi_{\mathrm{r}})}{\xi_{\mathrm{r}} - \xi_{\mathrm{l}}}, \tag{25}$$

$$c = \frac{2(a + \xi_{\mathrm{l}})}{\xi_{\mathrm{r}} - \xi_{\mathrm{l}}}. \tag{26}$$

Here $\xi$ may denote either of the streamwise, $x$, or wall-normal, $y$, spatial directions and $\xi_0, \eta_0$ are free parameters used to control resolution in critical flow areas. The chain rule is used in order to define collocation derivative matrices, $d/d\xi$ and $d^2/d\xi^2$, on the calculation grid $\xi$, given the collocation derivative matrices on the standard Chebyshev domain, $D \equiv d/d\eta$ and $D^2 \equiv D(D)$ [5], with the metrics of the transformation (23) calculated analytically.

Regarding boundary conditions for the basic flow problem, at the inflow boundary data is obtained from a boundary layer solution [22],

$$\zeta(x = x_{\mathrm{l}}, y) \equiv Z(y), \quad \psi(x = x_{\mathrm{l}}, y) \equiv \Psi(y). \tag{27}$$

At the outflow boundary, Briley's downstream boundary conditions,

$$\zeta_{xx} = \psi_{xx} = 0, \tag{28}$$

are used to close the system (20-21); in this case, no fringe treatment is required (i.e. $\lambda_f(x) \equiv 0$). Along $y$, the system (20-21) is closed by the boundary conditions

$$\zeta(x, y = y_\infty) = 0, \tag{29}$$

$$\psi(x, y = 0) = 0, \quad \psi_y(x, y = 0) = 0, \quad \psi_y(x, y = y_\infty) = \bar{u}(x, y \to \infty). \tag{30}$$

*Table 1.* Identification of the $x_0$ parameter range within which a steady laminar separation bubble forms. Howarth parameters taken $\beta_0 = 100, \beta_1 = 300$ and Reynolds number range examined $Re \in [10^3, 10^5]$. "inc" indicates incipient separation and "tp" stands for time-periodic flow.

| $Re_L$ | $10^3\times$ $\delta^*_{\text{infl}}$ | $Re_{\delta^*_{\text{infl}}}$ | $x_0$ | $t_\infty$ | Steady | LSB | $10^{-2}\times$ $\max\{\bar{u}_\infty\}$ | $10^2\times$ $\max\{\lvert\bar{u}_{\text{rev}}\rvert/\bar{u}_\infty\}$ | $\xi_{\text{sep}}$ | $\xi_{\text{reat}}$ |
|---|---|---|---|---|---|---|---|---|---|---|
| 5000 | 2.107 | 31.61 | 0.25 | 0.14 | y | n | 0.75 | - | - | - |
| 5000 | 2.107 | 31.61 | 0.26 | 0.15 | y | y | 0.74 | 0.009 | 0.1340 | 0.1848 |
| 5000 | 2.107 | 31.61 | 0.27 | 0.21 | y | y | 0.73 | 0.973 | 0.0986 | 0.2741 |
| 5000 | 2.107 | 31.61 | 0.28 | - | n | - | 0.72 | - | - | - |
| 10000 | 1.490 | 44.70 | 0.24 | 0.11 | y | n | 0.76 | - | - | - |
| 10000 | 1.490 | 44.70 | 0.25 | 0.15 | y | y | 0.75 | 0.227 | 0.0891 | 0.1687 |
| 10000 | 1.490 | 44.70 | 0.26 | - | n | - | 0.74 | - | - | - |
| 15000 | 1.216 | 54.72 | 0.23 | 0.09 | y | n | 0.77 | - | - | - |
| 15000 | 1.216 | 54.72 | 0.24 | 0.14 | y | y | 0.76 | - | 0.0795 | 0.1421 |
| 15000 | 1.216 | 54.72 | 0.25 | - | n | - | 0.75 | - | - | - |
| 20000 | 1.053 | 63.18 | 0.22 | 0.07 | y | n | 0.78 | - | - | - |
| 20000 | 1.053 | 63.18 | 0.23 | 0.09 | y | y | 0.77 | 0.007 | 0.0854 | 0.1070 |
| 20000 | 1.053 | 63.18 | 0.24 | 0.25 | y | y | 0.76 | 1.325 | 0.0637 | 0.1604 |
| 20000 | 1.053 | 63.18 | 0.25 | - | n | - | 0.75 | - | - | - |
| 20833 | 1.032 | 64.50 | 0.22 | 0.07 | y | n | 0.78 | - | - | - |
| 20833 | 1.032 | 64.50 | 0.23 | 0.10 | y | y | 0.77 | 0.023 | 0.0815 | 0.1111 |
| 20833 | 1.032 | 64.50 | 0.24 | 0.20 | y | y | 0.76 | 1.378 | 0.0607 | 0.1665 |
| 20833 | 1.032 | 64.50 | 0.25 | - | n | - | 0.75 | - | - | - |
| 30000 | 0.860 | 77.40 | 0.21 | 0.05 | y | n | 0.79 | - | - | - |
| 30000 | 0.860 | 77.40 | 0.22 | 0.07 | y | inc | 0.78 | - | - | - |
| 30000 | 0.860 | 77.40 | 0.23 | - | n | - | 0.77 | - | - | - |
| 100000 | 0.471 | 141.34 | 0.17 | 0.08 | y | n | 0.83 | - | - | - |
| 100000 | 0.471 | 141.34 | 0.18 | - | tp | n | 0.82 | - | - | - |

A documentation of the Howarth separated boundary layer flow for Briley's parameters $\beta_0 = 100$ and $\beta_1 = 300$ may be found in table 1; note that chord Reynolds numbers representative of flight conditions fall within the $Re-$range shown. The time lapsed until a steady state solution is obtained (when such a state exists) is denoted by $t_\infty$, $\bar{u}_{\text{rev}}$ is the recirculation velocity and $\xi_{\text{sep}}, \xi_{\text{reat}}$ are the streamwise wall coordinates of the streamline $\psi = 0$. A limited number of the available results at different Reynolds numbers is shown in the $x_0-$range around separation, alongside an indication whether a steady-state (attached or separated) exists and whether a steady LSB has been formed.

It is observed that $t_\infty$ is a function of $x_0$ but is independent of $Re$. Results well-known from other LSB model studies have been recovered in the present Howarth context, namely that the basic states are extremely sensitive to small parameter changes at all $Re-$values examined, and also that the appearance of steady LSB flow

is a low-Reynolds number phenomenon; evidence exists that beyond $Re \approx 3 \times 10^4$ either attached steady states (albeit mildly decelerated) or time-periodic shedding bubbles are the only flows that may be sustained. The time-dependence of the signal at an arbitrarily chosen field point is shown in figure 1 at $Re = 10^5$, both in its entire development in time and as a zoom into a short-time interval of several shedding periods. In a global instability analysis context, the loss of steady flow at a particular Reynolds number is an indication of global instability of the $\beta = 0$ direct BiGlobal eigenmode above this Reynolds number value and damping of the same mode below this threshold. Another interesting result is the shortening of the LSB with increasing Reynolds number, although the strength of recirculation does not appear to depend on $Re$. This latter result should be put in context by reference to analogous results in other LSB configurations, which monitor time-averaged, as opposed to steady laminar quantities. Quantification of these points, based on solutions of the direct EVP, is currently underway.

### 2.2. EVP Results

The classic square lid-driven cavity (LDC) has served as testbed of numerical algorithms for the solution of the incompressible equations of motion in two- and three spatial directions. The differences between the results of the two approaches (2-d solutions predict steady laminar flow up to $Re \approx 8500$ while 3-d flow becomes unsteady and turbulent at $Re \approx 1000$) have been identified independently by Theofilis [23] and Albensoeder, Kuhlmann and Rath [1] to originate in linear (modal) three-dimensional BiGlobal instability. BiGlobal instability in the lid-driven cavity is now well-understood, making this flow a good candidate in order to validate numerical solutions of the adjoint BiGlobal eigenvalue problem, unlike the LSB flow in which the demarcation between KH and global instability is presently not documented. It is well-known that the direct and adjoint eigenspectra are complex conjugates of each other; this result is clearly visible in figure 2, which shows the leading eigenvalues $\omega$ obtained from numerical solution of the direct (6-9) and the adjoint (15-18) EVPs at the critical conditions of LDC flow, $Re = 782.61, \beta = 15.37$. The region of maximum flow sensitivity, associated with the direct-adjoint product [14], is also shown in this figure. These results, as well as others in analogous flows not presented here, have verified and validated the numerical solution of (15-18) and build confidence in the capacity of the method to address the LSB flow control problem.

However, numerical solutions of the direct BiGlobal EVP in LSB flows, the basic states of which may be found in the results of table 1, have revealed the large resolution requirements for accurate description of convective instabilities, when these are recovered as BiGlobal eigenmodes [24]. On the other hand, the numerical solution of both the direct and the adjoint BiGlobal EVP relies on an iterative Krylov subspace iteration method which, in turn, solves a number of large linear systems equal to the subspace dimension. A key element of this process is a single LU-decomposition of the matrices which discretize the LHS of (6-9) and (15-18). The in-core storage of these matrices confines serial solution of the EVP problems to low resolutions, while the associated LU-decompositions are responsible for practically all the CPU time consumed in the Krylov iteration; on both counts, parallelization of the LU decompositions is a promising way forward. First steps, using up to 32 nodes (64

Myrinet-interconnected processors) and focusing on the solution of a single Poisson-based model linear system, have shown linear scaling of the wall CPU time with the number of processors [24]. At the same time, memory is distributed over all available processors, such that eventually the size of the BiGlobal EVP which can be solved will become a function of the number of processors available. Here, a further step is taken, which integrates the parallel linear-system solution methodology into an iterative, Arnoldi eigenvalue problem solution. Again, instead of targeting either of (6-9) or (15-18), a related EVP which preserves the essential BiGlobal EVP ingredient of the Laplacian operator is chosen, namely $\nabla^2 f = \lambda f$, for which the eigenvalues are analytically known [28]. Figure 3 shows the leading eigenvector of this EVP, obtained by parallelizing the Arnoldi algorithm and distributing the matrix which discretizes the nabla operator over four processors. All digits of the corresponding eigenvalue, $\lambda = 2\pi^2/4$, have been recovered correctly in double precision, while the (color-coded as *blue, red, green* and *cyan*) distribution of the eigenvector over the four processors is also visible. This result builds confidence in the parallel solution of the BiGlobal eigenvalue problems (6-9) and (15-18), which is also underway.

## Acknowledgements

The material is based upon work sponsored by the Air Force Office of Scientific Research, Air Force Material Command, USAF, under Grant number #063066 to *nu modelling s.l.*, entitled *Global instabilities in laminar separation bubbles.* The Grant is monitored by Lt. Col. Dr. Rhett Jefferies of AFOSR and Dr. S. Surampudi of the EOARD. The views and conclusions contained herein are those of the author and should not be interpreted as necessarily representing the official policies or endorsements, either expressed or implied, of the Air Force Office of Scientific Research or the U.S. Government.

## References

[1] S. Albensoeder, H. C. Kuhlmann, and H. J. Rath. Three-dimensional centrifugal-flow instabilities in the lid-driven-cavity problem. *Phys. Fluids*, 13(1):121–136, 2001.

[2] T. Allen and N. Riley. Absolute and convective instabilities in separation bubbles. *Aeronautical Journal*, 99:439–448, 1995.

[3] T. R. Bewley. Flow control: New challenges for a new renaissance. *Progress in Aerospace Sciences*, 37:21–58, 2001.

[4] W. R. Briley. A numerical study of laminar separation bubbles using the Navier-Stokes equations. *J. Fluid Mech.*, 47:713–736, 1971.

[5] C. Canuto, M. Y. Hussaini, A. Quarteroni, and T. A. Zang. *Spectral methods: Fundamentals in single domains.* Springer, 2006.

[6] S. S. Diwan, S. J. Chetan, and O. N. Ramesh. On the bursting criterion for laminar separation bubbles. In R. Govindarajan, editor, *Sixth IUTAM Symposium on Laminar-turbulent transition*, pages 401–407. Springer, 2006.

[7] A. Dobrinsky and S. S. Collis. Adjoint parabolized stability equations for receptivity prediction. AIAA Paper 2000-2651, 2000.

[8] M. Gaster. The structure and behaviour of separation bubbles. Technical Report 3595, NPL Rep. & Mem., 1967.

[9] F. Giannetti and P. Luchini. Structural sensitivity of the first instability of the cylinder wake. *J. Fluid Mech.*, 581:167–197, 2007.

[10] D. A. Hammond and L. G. Redekopp. Local and global instability properties of separation bubbles. *Eur. J. Mech. B/Fluids*, 17:145–164, 1998.

[11] D. C. Hill. Adjoint systems and their role in the receptivity problem for boundary layers. *J. Fluid Mech.*, (292):183–204, 1995.

[12] L. Howarth. On calculation of the steady flow in the boundary layer near the surface of a cylinder in a stream. *A.R.C. Reports and Memoranda*, 1632, 1934.

[13] L. Howarth. On the solution of the laminar boundary-layer equation. *Proc. R. Soc. Lond. A*, 164:547, 1938.

[14] P. Luchini. Adjoint methods in transient growth, global instabilities and turbulence control. Proc. *Global Flow Instability and Control Symposium II*, Crete Greece, 2003.

[15] P. M. Morse and H. Feshbach. *Methods of Theoretical Physics, Parts I, II.* McGraw-Hill, 1953.

[16] J. O. Pralits, A. Hanifi, and D. S. Henningson. Adjoint-based optimization of steady suction for disturbance control in incompressible flows. *J. Fluid Mech.*, (467):129–161, 2002.

[17] J.-Ch. Robinet. Bifurcations in shock-wave/laminar-boundary-layer interaction: global instability approach. *J. Fluid Mech.*, (579):85–112, 2007.

[18] J.-Ch. Robinet and P. Joubert de la Motte. Global instabilities in separated laminar boundary layer. Turbulence and Shear Flow Phenomena, TSFP-3, Sendai, Japan, June 25-27 2003, 2003.

[19] M. Simens, L. González, V. Theofilis, and R. Gómez-Blanco. On fundamental instability mechanisms of nominally 2d separation bubbles. In R. Govindarajan, editor, *Sixth IUTAM Symposium on Laminar-turbulent transition*, pages 89–95. Springer, 2006.

[20] P. R. Spalart. Direct numerical study of leading-edge contamination. CP-438 Fluid Dynamics of Three-Dimensional Turbulent Shear Flows and Transition, pages 5.1 – 5.13, Cesme, Turkey, 3–6 October 1988, 1988. AGARD.

[21] V. Theofilis. Global linear instability in laminar separated boundary layer flow. In H. Fasel and W. Saric, editors, *Proc. of the IUTAM Laminar-Turbulent Symposium V*, pages 663 – 668, Sedona, AZ, USA, 2000.

[22] V. Theofilis. Advances in global linear instability analysis of nonparallel and three-dimensional flows. *Prog. Aero. Sci.*, 39:249–315, 2003.

[23] V. Theofilis. Globally unstable basic flows in open cavities. *6th AIAA Aeroacoustics Conference and Exhibit*, AIAA-2000-1965.

[24] V. Theofilis. On instability properties of incompressible laminar separation bubbles on a flat plate prior to shedding. Number AIAA Paper 2007-0540, Reno, NV. Jan 5–8, 2007.

[25] V. Theofilis, P. W. Duck, and J. Owen. Viscous linear stability analysis of rectangular duct and cavity flows. *J. Fluid. Mech.*, 505:249–286, 2004.

[26] V. Theofilis, A. Fedorov, D. Obrist, and U. Ch. Dallmann. The extended görtler-hämmerlin model for linear instability of three-dimensional incompressible swept attachment-line boundary layer flow. *J. Fluid Mech.*, 487:271–313, 2003.

[27] V. Theofilis, S. Hein, and U.Ch. Dallmann. On the origins of unsteadiness and three-dimensionality in a laminar separation bubble. *Phil. Trans. Roy. Soc. London (A)*, 358:3229–324, 2000.

[28] L. N. Trefethen. *Spectral methods in Matlab.* SIAM, 2000.

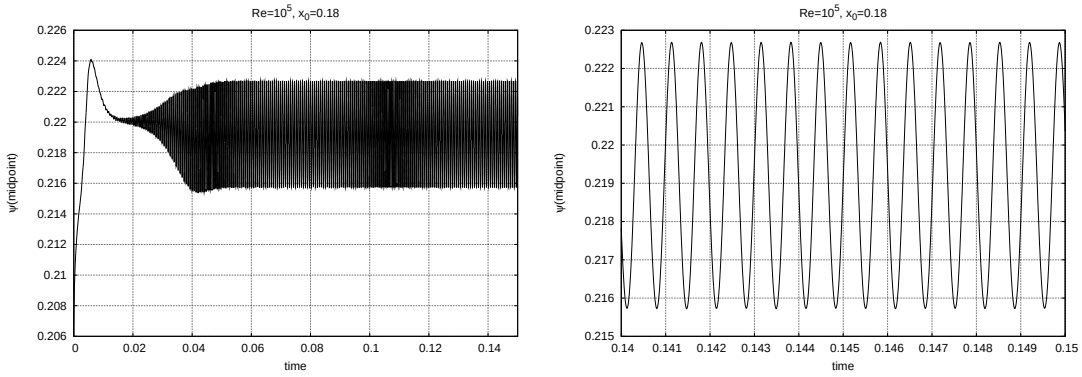


*Figure 1.* Dependence on time of the value of the streamfunction at an arbitrarily-chosen point in the calculation domain at $Re = 10^5$. *Left:* complete development, starting from rest until the establishment of shedding. *Right:* Detail of the shedding process.

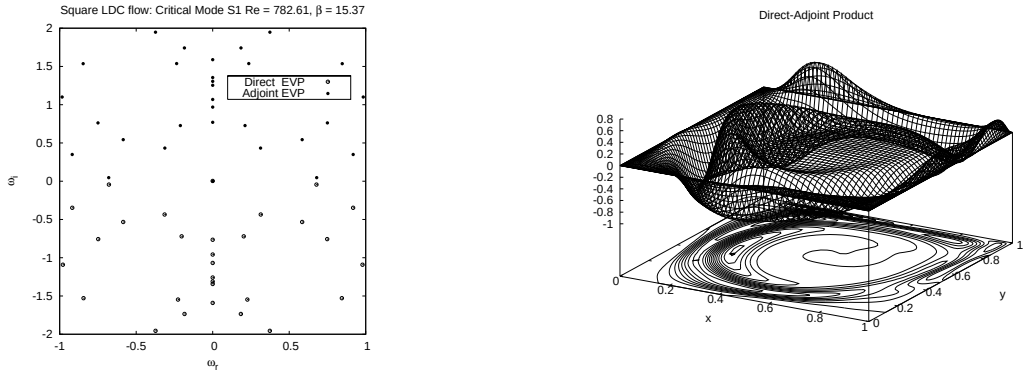


*Figure 2. Left:* Direct and adjoint eigenspectra in the neighborhood of $\omega = 0$ at critical conditions of the lid-driven cavity flow. *Right:* Direct-Adjoint product of the leading eigenmode [14, 9].

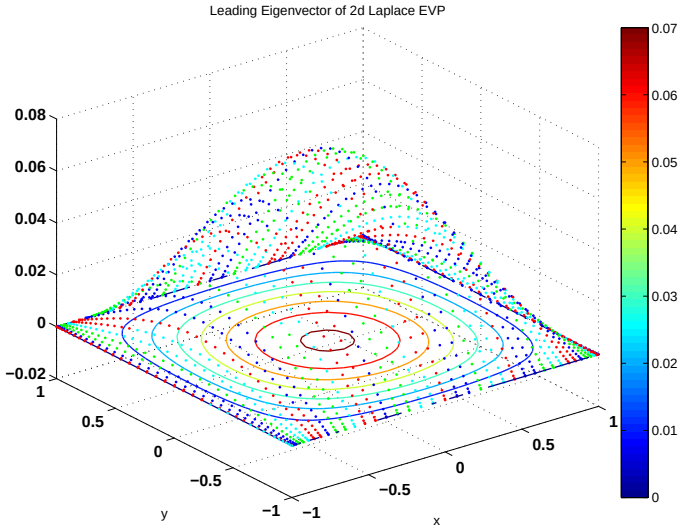


*Figure 3.* Parallel solution of the 2d Laplace EVP $\nabla^2 f = \lambda f$: leading eigenvector corresponding to the eigenvalue $2\pi^2/4$ (courtesy of Mr. D. Rodriguez)